ROSAT PSPC Observation of the NE Region of the Vela SNR: II. Spectral Analysis with a Non Equilibrium of Ionization Emission Model.

F. Bocchino, A. Maggio, S. Sciortino
Istituto e Osservatorio Astronomico di Palermo
Piazza del Parlamento 1, 90134 Palermo, ITALY

December 16, 1996

Submitted to ApJ

Abstract

We have developed a grid of Non Equilibrium of Ionization (NEI) models which depends on the electron temperature and ionization time, and which is suitable to be used for fitting X-ray spectra. Using this grid, we have carried out spatially resolved spectral analysis of a *ROSAT* Position Sensitive Proportional Counter (PSPC) observation of the North-East shock region of the Vela supernova remnant (SNR) on an angular scale of $10'$ (~ 1.0 pc at the distance of the remnant). The adopted model passes the χ^2 test at the 95% confidence level on the 45% of the considered spatial bins, giving unexpected low values of the ionization time ($\log \tau \sim 0-1$ yr cm^{-3}). We discuss the possibility that this result may be due to a reduced contribution from line emission, which may be related to locking of metals in grains. We also find significant temperature gradients on the scale explored, and we argue that they are correlated to ISM inhomogeneities encountered by the shock front. The emission from the remaining 55% of the bins is incompatible with the single-tau single-temperature NEI model, and a feasible description rests on the two temperature (2T) Collisional Equilibrium of Ionization (CIE) model we have adopted in our previous analysis of the same data set. We temptatively interpret our results in terms of superposition of shocks propagating in an inhomogeneous medium, which produces a multi-temperature and multi-ionization stage plasma.

1 Introduction

This is the second of a series of papers on a ROSAT PSPC observation of the NE shock region of the Vela SNR. In Paper I (Bocchino, Maggio and Sciortino 1994), we performed a spatially resolved spectral analysis using Collisional Ionization Equilibrium (CIE) plasma emission models: we showed that the X-rays originating from the shock front region cannot be described in terms of a single-temperature model, and that a second thermal component is required to give a statistically acceptable description of the observed spectra. This seems to be the case down to the smallest angular scale on which we were able to perform spectral analysis ($5'$, i.e. 0.5 pc at the distance of the SNR).

Accumulated evidence shows that the plasma of several SNR's is not in CIE. High spectral resolution X-ray observations of SNR's, such as those taken with the *Einstein* FPCS (for a review see Canizares 1983), have clearly shown, by detailed plasma diagnostics of He-like triplets, that the plasma dominating the emission, whether ejecta or swept-up interstellar medium, has not reached ionization equilibrium even in relatively old SNR. Apart from these high spectral resolution observations, which usually had low or none spatial resolution, the inclusion of relevant physical effects in the analysis of spatially resolved SNR X-ray emission, such as the non-equilibrium of ionization (NEI) or the ion/electron non-thermal equilibrium, has been traditionally prevented by the poor spectral resolution of imaging detectors (like *Einstein* IPC, *EXOSAT* LE+CMA, and HEAO-1 A2 experiments) as well as by the computational effort required to evaluate a model of the X-ray emission from a NEI optically thin plasma. Some efforts along this way have been made by Hamilton & Sarazin (1984), who created a grid of NEI emission spectra to be compared with spatially integrated remnant emission, by Hughes & Helfand (1985, hereafter HH85), who implemented a matrix algorithm approach for the solution of the population fraction equation in the NEI case, and by Masai (1984), who calculated the emission spectra (1-160 Å) in the transient phase of ionization. Masai

(1994) gave a detailed description of non-equilibrium processes in SNR, including NEI. As a result, the NEI nature of the X-ray emission of many SNR's has been temptatively established by simultaneous measurements of the spatially averaged temperature and ionization time, which do not in general provide detailed spatial coverage and resolution (e.g. Hwang et al. 1993).

More recent accurate NEI analysis of SNR data have appeared in the literature. For instance, Miyata et al (1994) reported on an ASCA observation of a small (22×22 arcmin^2) region in the NE Rim of the Cygnus Loop, and Hayashi et al (1994) examined the integrated spectrum of E0102-72. The availability of the *ROSAT* and ASCA missions to the scientific community now gives the opportunity to look in greater detail and with a greater physical consistency at the SNR X-ray emission, thanks to the improved spectral and spatial resolution. In fact, we are in the position to test the new picture being developed since early *Einstein* FPCS observations: the SNR's generally expand in a non uniform medium, the plasma is in NEI condition, the post shock metal abundances may not be the same as the cosmic values, and electrons and ions may have different temperatures. These effects cannot be overlooked when attempting to analyze spectra from current detectors and will certainly be important with future X-ray detectors on board SAX, Jet-X, AXAF and XMM. Moreover, since the NEI emission models take into account an additional physical effect with respect to CIE models, the results previously obtained on SNR's with CIE models should in principle be revisited.

In this paper we present the results of a spatially resolved spectral analysis of a ~ 3 square degree region in the NE of the Vela SNR, using a NEI emission model. We take advantage of the angular resolution of the *ROSAT* PSPC in order to resolve the temperature, density and ionization time distributions of the remnant, which is determined not only by the plasma dynamics but also by possible inhomogeneities present in the ISM.

In this context, the lack of a NEI thermal plasma emission model in the most widely used software packages (PROS, EXSAS, XSPEC) for the analysis of the

X-ray spectra is an obstacle to the widespread adoption of these more physical descriptions of the X-ray emission. To carry out this work, we have first developed a grid of NEI model spectra suitable to be used for fitting X-ray spectra. We have then used the grid to perform the spectral analysis of our data.

We will show that the single-ionization time, single-temperature NEI model we have developed (hereafter the STNEI model) provides a statistically acceptable description of the data for about 45% of the spatial bins analyzed. This result and the conclusions of Paper I tend to rule out the one-temperature nature of the X-ray emission of the Vela SNR shock region and leads naturally to a scenario with multiple shocks in an inhomogeneous medium, which could be quite common in middle aged SNR's.

Our paper is organized as follows: in section 2 the data are briefly reviewed, and in section 3 we discuss the basic assumptions for computing the STNEI plasma emission model we have adopted. In section 4 we describe the basic data analysis and in section 5 we give the results of the STNEI model fitting procedure. In section 6 we discuss the results of our analysis comparing them with previous results on the X-ray emission of the Vela SNR; finally, in section 7, we summarize our results.

2 Basic data

The observation of the NE rim of the Vela SNR ($\alpha(2000) = 8^h 44^m 24^s$, $\delta(2000) = -42°39'00''$) was performed with the *ROSAT* PSPC on 1991 April 25. The PSPC field of view is circular with $\sim 1°$ diameter. The spatial resolution is 30 arcsec FWHM at the center of the field of view and 2.7 arcmin FWHM at 45' off-axis. The spectral resolution is $E/\Delta E \sim 2$ at 1 keV. We collected 5×10^5 counts in 3944 seconds exposure time. The optimized time-screening algorithm described in Bocchino, Barbera & Sciortino (1996) for elimination of residual non-cosmic PSPC background was run on the data, resulting in the rejection of 186 seconds (5% of the exposure time).

For a more detailed description of the observation we refer to Paper I.

3 The Model

The first NEI models of a SNR X-ray emission can be found in Itoh (1979), Cox & Anderson (1982) and Hamilton, Sarazin and Chevalier (1983). They solve the NEI system of equations for each element in several concentric shells covering almost the whole remnant, and then integrate the emission over all shells to obtain the predicted NEI spectrum to be compared with observations, once folded with the instrumental response. Our data call for a more detailed approach for two main reasons: first, the clumpy nature of the emission from Vela SNR suggests expansion in a non uniform medium, which in turn requires spectral analysis to be performed on a small angular scale. Second, the high spatial resolution and high counting statistics of our observation allow us to split the 1° radius image in many spatial bins, and to perform separate spectral analysis on each of them. Because of the under-ionization of the plasma, the spatially resolved spectra of the shock region are expected to differ considerably from either the spectra of the central region or the overall integrated spectrum of the SNR (Brinkmann, 1988).

3.1 Dynamical model

We adopt the Sedov-Taylor dynamical model of an adiabatically expanding spherical blast wave (Taylor, 1950; Sedov, 1959) appropriate for middle-aged SNR's. In such a model the solution for the temperature and density has a self-similar form, and the radius of the shell and the shock velocity evolve with time as $t^{2/5}$ and $t^{-3/5}$, respectively. The Sedov solution is a good approximation when the swept up interstellar mass exceeds the mass of the SN ejecta ($M_{swept} > M_{ejecta}$, Woltjer 1972). The association between the Vela SNR and the old pulsar PSR0833-45 (Weiler & Panagia 1980, Weiler & Sramek 1988) suggests that the SNR is well in its adiabatic phase. To our purposes, a useful relation linking the shock temperature T_s with the shock wave velocity v_s is the following (McKee & Hollenbach 1980):

$$T_s = \left(\frac{v_s}{839\ km/sec}\right)^2 \times 10^7\ K \propto t^{-6/5}. \quad (1)$$

In the following, we shall assume instantaneous energy equipartition between ions and electrons at the shock front. In this case, eq. 1 allows us to derive the shock speed from X-ray observations; in fact, the electron temperature derived from fitting the X-ray data is equal to T_s in equation 1.

3.2 Emission Model

The expanding shock wave continuously encounters neutral ISM. Thermodynamical quantities just before and after the shock are linked by the Rankine-Hugoniot conditions (Landau & Lifshitz, 1974). Typical post shock temperatures of middle-aged SNR's range between $10^6 - 10^7$ K and the plasma can be considered optically thin. Detailed calculations of X-ray spectra are difficult because of the uncertainties of ionization and recombination rates of relevant elements. One of the most widely used emission codes is described in Raymond & Smith (1977). Differences in the input atomic physics rates lead to differences in computed spectra; for a discussion of the impact of the differences among spectral codes on spectral analysis of PSPC data, see the Appendix of Paper I.

(a) Non Equilibrium of Ionization

The plasma CIE emission models assume the local equality of the electron kinetic temperature, T_e, and the ionization temperature, T_I, defined in terms of the ions population fractions. Because of the collisional nature of the ionization process, if a perturbation makes T_e and T_I different, the equilibrium is restored on a time scale t_{eq} depending on electron kinetic temperature T_e through the ionization and recombination rates. In the case of middle-aged SNRs, we have $T_e = 10^6 - 10^7$ K and $T_I(t=0) \simeq 10^4$ K, since before the shock the ISM is in CIE condition at $T_e \simeq 10^4$ K. Hence, the post-shock plasma is under-ionized, and, for any given element, we have

$$t_{eq}(T) \geq \sum_i (n_e C_i(T))^{-1} \quad (i = 1, 2, ..., M). \tag{2}$$

where n_e is the electron density, C_i the ionization rates and M is the most abundant ionization stage in condition of CIE at the temperature T (we assume that ions $1, ..., M-1$ are completely ionized). For instance, with $T_e = 3 \times 10^6$ K, $n_e = 0.2$ cm^{-3} we have $t_{eq} \geq 10^4$ yr for Carbon, 2×10^4 yr for oxygen, and 3×10^3 yr for iron. A more detailed calculation of t_{eq} is given by Masai (1994). These estimates imply that we expect the plasma to be in CIE at a distance $\Delta_{eq} \geq t_{eq} v_r$ behind the shock, where $v_r = v_s/4$ is the plasma velocity relative to the shock. In the case of the Vela SNR, where $v_r \sim 400/4$ km sec^{-1}, $\Delta_{eq} \geq 0.3$ pc for iron, and $\Delta_{eq} \geq 2.2$ pc for oxygen. Note that this is a strict lower limit because this simple reasoning does not take into account the shock deceleration. In conclusion, a NEI treatment is required to properly model the Vela SNR X-ray emission.

(b) The STNEI emission model

To properly model the X-ray spectra from the observed shock region of Vela SNR, we have built a grid of NEI spectra with two free parameters: the electron temperature, T_e, and the ionization time τ,

$$\tau = \int_0^{t_{now}} n_e dt \tag{3}$$

where $t = 0$ is the time when a small volume of plasma, of which we want to find the emission, is struck by the blast wave. Keeping fixed the plasma element abundances, T_e, τ and a normalization factor, depending on the plasma density, are the only parameters which a NEI spectrum depends on. To solve the problem of computing NEI X-ray emission we have made two main assumptions:

1. We assume that once a small volume of plasma is struck by the blast wave, it moves rigidly within a region of constant density and temperature. In other words, we neglect the convective terms in the continuity equation of the population fraction. This is certainly a good assumption in the Sedov expansion phase, since matter moves rigidly with a speed equal to $\frac{3}{4}v_s$, but it could result

not valid in case of ISM inhomogeneities with high density contrast. A more general approach should take into account the change in ionization structure due to displacement of the plasma moving across zones with different thermodynamical conditions. Such an approach, that requires a more general code, is under study and will be reported in a subsequent paper.

2. The electron temperature, T_e, and density, n_e, stay constant during the ionization process. This is equivalent to assume that the emerging spectrum depends only on the instantaneous electron temperature and density. This assumption has been discussed by Hamilton & Sarazin (1984) and is valid when the ionization rates vary slowly with temperature, i.e. in high temperature conditions, or alternatively when the analysis is limited to the shock region, since the Sedov model predicts slow variations in the region few parsecs behind the shock front of a Vela-like SNR (Itoh 1979, Cui & Cox 1992). This approximation is no longer valid when one considers the central regions of SNR's. Again, problems may arise if a ISM cloudlet with high density gradient is shocked by the blast wave, because strong temperature and density gradients will occur in the subsequent cloud evolution (Bedogni & Woodward, 1990).

An approach similar to our was used by HH85 in developing their NEI code based on matrix calculations. Our calculation scheme is also applicable to physical conditions with time-dependent temperature and density profiles. Although we have assumed constancy in this work, we plan to generalize our model to deal with such time-dependent physical conditions.

Throughout all our calculations, we used the Exchange Classical Impact Parameter (ECIP) rates (Summers, 1974, Raymond & Smith, 1977), which are more accurate, especially in NEI conditions, than the Lotz formula (Lotz, 1967) and the related ionization rates (Mewe & Groneschild, 1981, Shull & van Steenberg, 1981), as discussed by Hamilton, Sarazin and Chevalier (1983).

We have solved the population equations for ions of the most abundant cosmic elements (He, C, N, O, Ne, Mg, Si, S, Ar, Ca, Fe, Ni) using a fifth order Runge-Kutta method (Press et al. 1986) modified to take into account specific physical events and numerical problems like ions turning on and the "stiffness" of the involved equations. The initial condition ($\tau = 0$) is the impact between the blast-wave and the small volume of plasma. We have assumed that the ISM elements are all neutral at this time. We have also checked that the results of our spectral analysis are not affected by this choice: in particular, the spectral fitting results obtained with grids of spectra computed assuming ISM initial temperatures up to 10^4 K do not differ appreciably from results obtained with our choice. Once the ionization stages have been found for a given couple of values (T_e, τ), we have inserted the ion relative abundances into the Raymond-Smith code (Raymond & Smith, 1977, Raymond, 1989) to compute the final spectrum which was saved as a table readable by the XSPEC spectral fitting code. The energy range of the synthetic spectra is 0.05-3 keV with a step of 0.007 keV, and the bin sizes of the STNEI emissivity table have been chosen in the following way: from 0.02 to 2.0 keV in steps of 0.02 keV for the temperature, and from $10^{-0.3}$ to $10^{5.0}$ yr cm^{-3} in logarithmic steps of 0.21 for the ionization time.

In order to test our capability to recover the original input plasma parameters when fitting *ROSAT* PSPC data with our STNEI model, we have performed several simulations of spectra in NEI conditions folded through the PSPC response, using various values of τ and of the number of total counts (Bocchino, Maggio & Sciortino 1996). On the basis of the fits of these simulated spectra, we concluded that optimal restoration of the free parameters T and τ is obtained using spectra with at least ~ 5000 counts in the PSPC band (0.1-2.4 keV).

By comparing the results produced by the Raymond-Smith code in CIE conditions and the results of our numerical calculations, we have also verified that the code we developed correctly describes the asymptotic behavior of the ionization process. In fact, the CIE population fractions are reproduced by our code when $\log \tau \gtrsim 5$ (in yr cm^{-3}).

(c) General considerations on the single-tau single-temperature NEI approach

We expect that, in each of our bins, the ionization time of the emitting plasma ranges from $\tau = 0$ at the shock front to $\tau = \tau_{max}$, corresponding to the most internal regions along the line of sight. It is not obvious that the PSPC spectra, including contributions from regions with different ionization times, can be described in terms of our single-tau single-temperature (STNEI) emission model, but we show in the following why such a description is likely feasible.

In order to estimate to which extent a STNEI model is appropriate in fitting spatially resolved spectra, we should take into account the variation of $P(T, \tau)$, and of the emission measure profile along our line of sight, since the plasma is optically thin.

Expected τ_{max} value. The expected value of τ_{max} depends on the spatial bin considered. Assuming $\tau = 0$ at the outer edge of the most external annulus (annulus 7, see section 4.1 and figure 2), a shock speed $v_s \sim 400$ km/sec, a post-shock density $n \sim 0.2$ cm^{-3} (see §5.1 and 5.3) we have $\tau_{max} \sim 6000$ yr cm^{-3} for a 1 pc wide spherical shell whose external edge matches the shock position. More internal shells do not scale linearly because the shock decelerates, but in any case τ_{max} should not be less than 6×10^3 yr cm^{-3} in the outermost zones, and it is not greater than a few $\times 10^4$ anywhere within the Vela SNR.

The NEI plasma emissivity. The X-ray emissivity in the *ROSAT* PSPC band is a strong function of τ. This is shown in Figure 1, which indicates, in the case of $kT = 0.2 - 0.3$ keV, variations of a factor of 7 between the maximum emissivity (at $\log \tau \sim 1.5 - 2.0$) and the emissivity in equilibrium condition ($\log \tau \sim 5$), and a factor of 30 between the maximum value and the value at $\log \tau \sim 0$.

Emerging spectrum of a Sedov SNR. The knowledge of the STNEI emissivity is not sufficient to characterize the emerging spectrum: the emission measure and ionization time distributions inside the remnant need to be estimated. Profiles of τ, density and temperature have been extensively derived in the case of Sedov solution and volume integrated emission. Hamilton & Sarazin (1984) worked on the characterization of NEI integrated spectra. They clearly show that, given a snapshot of a SNR, profiles and thermal history can be safely ignored when interpreting volume integrated spectra, since the only relevant "observational" parameters are the emission measure-weighted T_{av}, τ_{av} and the total emissivity, ϵ_{tot}. As they puts it, " ... Sedov type SNR will have similar spectra if they have the same T_{av}, τ_{av} and ϵ_{tot}". This is essentially due to the fact that most of the emission originates from a thin post-shock layer corresponding to a density bump (see also Cui & Cox 1992). We expect that these considerations can be applied also to our spatially-resolved analysis, because the contribution to the observed emission in each spatial bin, due to different layers along the line of sight, is similar but certainly less complex than in the case of the volume-integrated analysis.

The usage of a single component STNEI model as the one we have developed is therefore justified to some extent, and should provide us with a reasonable estimate of T_{av} and τ_{av}. We intend to further investigate this point using simulations in which Sedov STNEI spectra, integrated along the line of sight across a spherical emitting Sedov type SNR, are fitted with our STNEI model (Bocchino et al. 1996, in preparation). This approach will help us to understand how the best-fit values compare with the true local values of T and τ.

Alternative approaches. The justification of a STNEI model, even though not discussed in detail, is implicitly assumed in the literature. Single T - single τ fits were carried out with models very similar to our by, for instance, Hwang et al. (1993) and Yamauchi et al. (1993), and give typical $\log \tau$ values (in yr cm^{-3}) in the range 2.5-4.0 together with an estimate of the metal abundances in N132D and RX04591+1547 respectively. Fitting to linear combinations of STNEI models are not feasible as an alternative approach for fitting purposes, because of the large number of free parameters. In fact, for each component of the combination we should let vary at least the temperature and the normalization, but PSPC data are not suited for fitting with more than 4 or 5 free parameters. For the same reason (limited data quality), a different approach based on the computation of the distribution of T and τ by deconvolution of the data is unfeasible as well.

In summary, in spite of the mentioned simplifications reflecting our limited knowledge of the SNR plasma thermal history, our STNEI model is a more realistic description than the ionization equilibrium model we have considered in Paper I. A similar model was also adopted by Vedder et al. (1986) to analyze *Einstein* FPCS observations of the Cygnus Loop, and by Hughes & Singh (1994) to determine the abundances in the G292.0+1.8 SNR.

4 Data Analysis

4.1 Spatial grid resampling

In Bocchino, Maggio & Sciortino (1996) we show that a PSPC spectrum must have a few thousand counts in order to avoid secondary minima problems in the χ^2 space when fitted with our STNEI emission model. This effect is mainly due to the moderate PSPC spectral resolution. Since 98% of the $5' \times 5'$ spatial bins used for CIE spectral analysis in Paper I contained less than 5000 counts, a spatial rebinning of the data was necessary in order to use our STNEI 1T model. The new grid we have adopted (Figure 2a) contains 48 non empty bins (versus the 273 bins of Paper I) with angular size of $\sim 10' \times 10'$ and an approximate real size of 1×1 pc (cf. $5' \times 5'$ and 0.5×0.5 pc in Paper I). It contains only 12 bins (25% of the total) with less than 5000 counts (6 with less than 3000 counts) and it is a good compromise between spatial resolution and statistics.

The spatial bin layout has been tailored to study the radial profile of the plasma thermodynamical parameters derived from the fits (see Figure 2a). In fact, each spatial bin is the intersection of an annulus at a given distance from the Vela pulsar and a circular sector with its vertex on the pulsar. For a large scale view of the Vela SNR and the position of our pointed observation, see Figure 1b (Plate 11), in Paper I. In Table 1 the number of counts in each bins is reported, as well as the distance of the chosen annuli and their position angle.

4.2 The fitting process

We have taken into account vignetting corrections as well as the March 1992 version of the PSPC response matrix (see Paper I for further details about using this matrix). Moreover, we have taken into account the systematic errors of the adopted response matrix computed in the Appendix of Paper I by adding them in quadrature to the statistical errors. This procedure is required because of the high number of counts in the PSPC spectral channels. In the fitting process, we let T_e and τ vary, as well as the normalization that provides directly a measure of emission measure and, less directly (see below), an estimate of plasma density. Moreover, we have included as a free parameter the hydrogen column density N_H. We have considered the PSPC channels in the range 3-30, since channels 31-34 (corresponding to energies in the range 2.02-2.48 keV) have too few counts for the validity of the χ^2 statistics in the fitting (see Figure 3 as an example). With this choice, the number of degrees of freedom is 24.

This parametric fit approach is expected to give reliable results since: (i) the high statistics of our data allows us to determine parameters with quite small uncertainties (see Table 2); (ii) line strengths in the X-ray domain are strongly dependent on the ionization time (Figure 1; see also Brinkmann 1988) and this effect on the spectrum is measurable even with a low energy resolution detector like the *ROSAT* PSPC (Bocchino 1993). Since the results of the fitting procedure in some cases depend on the initial parameters guess, we have taken care of doing several trials with different starting points for the fitting to avoid convergence to local minima.

In summary, if we adopt the 95% confidence level (i.e. $\chi^2 > 36.4$ with 24 degrees of freedom), the model is acceptable in 21 spatial bins, most of which are located around positions *g3* and *e6* (Region E,F, and G in Paper I), whereas is rejected in the remaining 27 bins, like *d3, b5, d5* (Region C, H and A in Paper I). In the χ^2 map (Figure 2b), we show only those spatial bins where our STNEI model is acceptable; the remaining bins are not displayed.

In Figure 3, we show spectra and best-fit STNEI models for two sample bins where we found acceptable χ^2 values (*e6*, $\sim$ 9000 counts; *c7*, $\sim$ 2600 counts) but different parameter values (T = 0.15 keV, $\log\tau \sim 0$ in *e6* and T = 0.21 keV, $\log\tau \sim 5$ in *c7*). The unfolded model spectra are also shown in the right-hand panels, and indicate the different contribution from the line emission to the total X-ray emissivity in the two cases. In Figure 4, we show an example of spectrum which could not be fitted successfully (*d3*, 15200 counts): in this bin our model underestimates the observed spectrum in the 0.6-1.0 keV energy range, and this characteristic is common also to other spectra with unacceptable χ^2 values.

In Table 2 we summarize the statistical errors associated to T and $\log\tau$, computed at the 99% confidence level in the case of two interesting parameters (Lampton, Margon & Bowyer 1976).

5 Results

5.1 Temperature Map

The temperature map is shown in Figure 5a. Temperature variations are within a factor of 3 across the whole image and within a factor 1.7 considering only the spatial bins with acceptable χ^2 values. These variations are statistically significant being larger than the fit uncertainties (see table 2). The temperature map reflects the different nature of the X-ray spectra of different regions in the field of view as already reported in Figure 2 of Paper I. The bins with acceptable values of χ^2 have temperatures in the range 0.15-0.25 keV ($1.8 - 2.9 \times 10^6$ K), which correspond to a shock speed of 350-450 km sec^{-1} (see Eq. 1). The spatial bins with high χ^2 are mostly concentrated in sectors a to d (e.g. *a4, a6, b5, d3*). We have verified that a 2T CIE model provides always a good fit to the observed spectra in the latter cases, in agreement with the results already found in Paper I.

5.2 Ionization time map

The resulting $\log \tau$ map is shown on Figure 5b. For each of the 21 bins where the STNEI model provides a good description of the observed spectra, we evaluated the confidence regions in the $T - \tau$ plane. The results indicate a value of the ionization time ≤ 10 yr cm^{-3} in 18 bins, while values compatible with the range $10^{2.5} - 10^5$ can be found in the remaining 3 cases.

The low τ values resulting in the other 18 bins is very difficult to interpret on the basis of our physical expectations, as discussed in section 3.2.c. In fact, we recall that, since our τ measurement is actually an estimate of τ_{av}, a ionization time less than 10 yr cm^{-3} can be regarded as unrealistic. Hence, in the next section, we will focus our attention only on the 3 bins which have a 99% confidence $\log \tau$ range which overlaps with the physically plausible range $1.0 < \log \tau < 5.0$ in yr cm^{-3}. In table 3, we list the 3 bins which satisfy this criterion (hereafter the T3 bins), and which therefore provide the most reliable numbers for the derived quantities.

5.3 Emission measure, density and pressure

As a result of the fitting procedure, we obtain a normalization factor for each spatial bin, NF, defined as:

$$NF = \frac{\int n_e^2 dV}{4\pi D^2} = \frac{\int n_e^2 A dl}{4\pi D^2} = \frac{\Theta}{4\pi} \int n_e^2 dl \; cm^{-5} \tag{4}$$

where D is the distance of the source, V is the volume of the emitting plasma element whose section perpendicular to the line of sight is A, and whose extension along the line of sight is l, and Θ is the subtended solid angle (in steradians). It is important to stress that NF does not depend on distance, unless the source fills less than the instrumental beam (as in the case of a point source, for example); this has the important consequence that a reliable estimate of SNR density can be derived from the X-ray observation, as we shall see below. Since the bins are spatially independent (i.e. their size is less than the width of the PSPC Point Spread Function), we can treat the emitting plasma in each pixel as an independent source.

In our case, $A = 10' \times 12'$, and an estimate of l is required to compute the density; this estimate can be obtained if we assume that the remnant is approximately spherical, as Aschenbach (1993) suggests, and if we further assume that the emission originates from a thin ($\Delta R/R = 12$) shell (the spherical shell model). In this case, l is a cord section,whose length is know analytically. The spherical shell model is suited for middle-aged SNR's expanding in a homogeneous medium, but it could run into problems if there are many clouds. Nevertheless, n_e depends weakly on l ($n_e \propto l^{-1/2}$), and possible deviations from the ideal case are not so important.

Following the above hypothesis, we have computed the post-shock density in the T3 bins (table 3) and the pressure. The latter was computed considering the plasma as a perfect gas, with equation of state $P_{gas} = 2n_e kT$. We estimate an error of 25% on the density and not more than 50% on the pressure. Assuming a compression factor of 4, we derive, from post-shock density values reported in Table 3, a pre-shock density of 0.03-0.05 in the T3 bins.

6 Discussion

The most important results of the STNEI (this work) and CIE (Paper I) spatially resolved spectral analysis are: 1) the one temperature models fail to fit the data as a whole; 2) in those cases where the 1T STNEI model is appropriate the resulting ionization time is unexpectedly low; and 3) a 2T CIE model is usually adequate.

The first and third point were already reported in Paper I, where we analyzed the same data set using CIE models. Indeed, Itoh (1979) suggested that the X-ray spectrum of a hot plasma in NEI condition could be approximated by a two temperature CIE plasma model. Therefore, on the basis of the results reported in Paper I, a single component nature of the X-ray emission could not be definitely excluded. As we have seen in the previous section, when considering the new results of the STNEI spectral analysis, we find that the 1T STNEI model fails in the same location where the 2T CIE model was appropriate (for instance, consider the *d3* bin and zone C in Paper I, or *b6* and zone H in Paper I). However, this does not necessarily imply that the Itoh suggestion is wrong in our case: the NEI model used by Itoh for synthesizing the X-ray SNR emission was different from our STNEI model, because it was a sum of Sedov shells with different τ values. Nevertheless, we interpret our results as a growing evidence that the medium in not homogeneous. If the medium was really homogeneous and the Sedov solution applied, then the peak in the NEI plasma emissivity (Fig. 1) and the peak in the Sedov density profile would yield a spectrum very similar to a STNEI spectrum, given the moderate PSPC spectral resolution.

We stress here that, in spite of the high counting statistics of our spectra, these results are not affected by uncertainties in the detector response, since they have been studied (Appendix A of Paper I) and accounted for by inclusion of systematic errors in the analysis.

6.1 Ionization Time and nature of the X-ray emission

The ionization time derived by fitting with STNEI model is quite low. Even considering the largest value allowed by the statistical confidence regions, τ appears to be not larger than 10 yr cm^{-3} in 18 out of 21 acceptable bins. The calculations of Itoh (1979) show that the ionization balance is very far from equilibrium near the shock front, but such a low range of τ can be regarded as unusual. We stress that the value we find is actually a weighted average of τ along the line of sight. Moreover, applying the analysis of Masai (1994) to the case of the Vela SNR, we expect $\log \tau \sim 3.5$ yr cm^{-3} (eq. 24 and Figure 5 of Masai 1994) in the thin shell responsible of most X-ray emission. There is still a chance that this could be due to the simplifications introduced in our modeling: in fact, Itoh (1979) shows that the population of some ions (e.g. O VI, O VII and some N and Ne) can remain far below the equilibrium just behind the shock front, weakening the strong O VII (0.57 keV) and O VIII (0.66 keV) lines and resulting in a low values of τ if derived from soft X-ray spectra. Nevertheless, a recent estimate of the ionization time in the shock region of the Cygnus loop based on a ASCA observation (Myata et al.

1994) gives $\tau \sim 10^3$ yr cm^{-3}, a value that has generally been found also in younger SNR's (Hughes & Singh, 1994). In particular Myata et al. (1994) found that a cosmic abundance STNEI plasma emission model is not sufficient to describe the spectrum, but underabundances of metal ($\sim 1/10$ of the cosmic values) should be taken into account. Moreover, Myata et al. have also found that a model based on a thermal bremsstrahlung plus 10 lines in the band 0.5-2.2 keV gives a description of the ASCA SIS spectrum of the Cygnus Loop as good as an optically thin STNEI plasma model.

For a better understanding of our results, taking also into account the above-mentioned recent ASCA results, we recall that our PSPC data can be also fitted by a bremsstrahlung model and by a two temperature Raymond-Smith model (Paper I). The NEI spectrum of an optically thin plasma with $\tau = 1 - 10$ yr cm^{-3} has the line contributions largely reduced, but not completely suppressed as in the case of the thermal bremsstrahlung. Based on the present results and those of Paper I, we conclude that more than one temperature and density component are likely contributing to the X-ray emission of the Vela SNR shock region we consider. The components are possibly both in NEI condition, but the limited spectral resolution of the *ROSAT* PSPC prevents us from testing this hypothesis. presence of two NEI temperatures.

The single temperature STNEI conditions are excluded as a general feature of the portion of the Vela SNR we considered, but they could be valid from a statistical point of view if applied locally in 21 spatial bins, mostly located in regions *e1*-*e7* and *f1*-*f7*. n these regions, the observed value of $\log \tau$ is mostly in the range 0-0.5. This derived ionization time is not realistic because we expect to see plasma with higher $\log \tau$ (§3.2), and Figure 1 shows that the NEI emissivity peaks at $\log \tau \sim 2$. At $\log \tau \sim 0$ the emissivity is more than 10 times less then the maximum value and should not contribute significantly to the total emission. Therefore, we have further investigated the issue of the reduced line emission contribution. In particular, we note that if the plasma has reduced metal abundances and we fit it with models having metal abundances fixed to cosmic values (as our STNEI model) using moderate spectrally resolved data, the result is an underestimate of the ionization time. In fact, our model predicts a steady evolution of the neutral plasma toward CIE conditions over long time scales. In the early stages of this process, ($\log \tau \simeq 0 - 1$) the contribution of line emission in the 0.1-2.4 keV band might be reduced, either because lines from low ionization stages have energy < 0.1 keV, or because the population of typical *ROSAT* band emitting ion species (like O VII) is intrinsically very low. The latter situation could arise as well in low abundance plasma in more advanced stages of ionization (e.g. $\log \tau \simeq 3$).

Recently, Vancura et al. (1994) have pointed out that the grains present in the ISM could survive long in the post-shock regions of SNR's under certain conditions of temperature and density (this is referred to as "the dusty shock model"). Since a non negligible fraction of the metals is locked up in the grains, they would not contribute to X-ray emission until they are released upon grain destruction; the plasma in the post-shock region could then have effectively reduced metal abundances. For instance, according to Vancura et al. (1994), the fractions of Fe, Si and O (whose lines mostly fall in the 0.1-2.4 keV band) locked up in grains in the ISM are respectively of 0.98, 0.98 and 0.2, and grain destruction doesn't change significantly the fractions before $\sim 8,000$ yr for a shock speed of 400 km/sec, similar to the shock speed we have derived. During this time, the shock has moved across a region of 3 pc, spanning about half of our FOV. So it is reasonable to conclude that our results may somehow be affected by grain depletion. Detailed comparisons between the dusty shock model and our data are not feasible at the moment because of the clumpy nature of the plasma in this region.

The results presented in this work and in Paper I leave open two explanations, namely, the effect of grain depletion in the PSPC spectra of SNR's and the presence of at least two phases in the post-shock medium. Given the old age of the Vela SNR and therefore the lack of reverse shocks due to stellar ejecta, the most immediate interpretation of the multi temperature nature of the X-ray emission could be the expansion of the blast-wave in an inhomogeneous medium with formation of multiple secondary shocks in an optically thin environment. This will be studied with a greater detail and with the aid of numerical simulations in a following paper.

7 Summary and conclusion

We have performed spatially resolved spectral analysis of a 1° radius field in the NE shock region of the Vela SNR, using a pointed PSPC observation and a STNEI emission model we developed. We have derived maps of temperature and ionization time with a spatial resolution of $\sim 10'$. The maps show that variations of thermo-dynamical parameters exist on this scale. The hypothesis that the X-ray emission could be described everywhere by a single-tau single-temperature STNEI model with cosmic abundances is rejected, but 21 out of 48 spatial bins have acceptable χ^2 values ($\chi^2 < 36$ correspondent to the 95% confidence level). Most of these 21 bins shows unexpectedly low values of the ionization time ($\log \tau \sim 0 - 1$ in yr cm^{-3}). Only 3 bins have acceptable χ^2 *and* a reasonable $\log \tau$ value (> 1.0). Considering this results and those presented in Paper I, where we show the success of the 2T CIE model on the same data set, a multi-phase description of the emitting plasma, probably due to superposition of multiple shocks in an inhomogeneous and optically thin medium, is needed for a valid interpretation of the observed spectra. Low metal abundances cannot be excluded because this could explain the low values of the ionization time derived assuming cosmic abundances. Deep optical observations in Hα and other "cooling" lines would be useful to confirm such a scenario, since ionizing material is expected to emit at Hα 6563 Å (Raymond, 1988) and cloudlets are expected to cool behind the shock and emit strongly in the optical band (McKee & Cowie, 1975). We have carried out such optical follow-up observations using the ESO-MPI 2.2m telescope at La Silla (Chile), which we shall report in a subsequent paper in this series.

Future planned extensions of this work will explore the abundances effect in the PSPC spectra, taking into consideration the recent findings of Vancura et al. (1994).

We intend also to study the physical conditions arising from a shock expansion in a inhomogeneous medium using the 2D Palermo hydrodynamical code (Reale, Peres and Serio, 1991) coupled to an appropriate NEI emission code. We think that such an approach may contribute to understand better our data and, more in general, to interpret of the SNR X-ray data of *ROSAT* as well as of future detector with higher spatial and spectral resolution. Moreover, more realistic effects in the STNEI model itself as outlined in section 3.2 are still to be considered.

Acknowledgement: F. Bocchino wishes to thank stimulating discussion with O. Vancura and the Supernova Remnant Group at CfA in Cambridge, USA. The authors wish to thank the suggestion and comments from S. Serio, R. Pallavicini, F. Reale and G. Peres. We also thank the referee, D. Cox, for his constructive criticism about the manuscript. This work was partially supported by Ministero della Università e delle Ricerca Scientifica e Tecnologica, GNA-CNR and a contract of Italian Space Agency (ASI).

References

Aschenbach, B. 1993, Adv. Space Res., 13, 1245-1255

Bedogni, R., & Woodward, P. R. 1990, A&A, 231, 481

Bocchino, F. 1993, Thesis, University of Palermo

Bocchino, F., Maggio, A., & Sciortino, S. 1994 (Paper I), ApJ, 437, 209

Bocchino, F., Barbera, A., & Sciortino, S. 1996, Proceedings of "RöntgenStrahlung from the Universe", Wurzburg (Germany), eds. H. U. Zimmermann, J. E. Trümper & H.York, MPE Report 263, 673

Bocchino, F., Maggio, A., & Sciortino, S. 1996, Proceedings of "RöntgenStrahlung from the Universe", Wurzburg (Germany), eds. H. U. Zimmermann, J. E. Trümper & H.York, MPE Report 263, 235

Brinkmann, W. 1988, in Supernova Shells and Their Birth Events, Kundt W. ed., Springer - Verlag

Canizares, C. R. 1983, in Supernova Remnants and Their X-ray Emission, eds. Danzinger & Gorenstein, 205

Cox, D. P., Anderson, P. R. 1982, ApJ, 253, 268

Cui, W., & Cox, D. P. 1992, ApJ, 401, 206

Gorenstein, P., Harnden, F. R. Jr., & Tucker, W. H. 1974, ApJ, 192 661

Hamilton, A. J. S., & Sarazin, C. L. 1984, ApJ, 284, 601

Hamilton, A. J. S., Sarazin, C. L., & Chevalier R. A. 1983, ApJS, 51, 115

Hayashi, I., Koyama, K., Ozaki, M., Miyata, E., Tsunemi, H., Hughes, J. P., & Petre, R. 1994, PASJ,46, L121

Hughes, J. P., & Helfand, D. J. 1985, ApJ, 291, 544

Hughes, J. P., & Singh, K. P. 1994, ApJ, 422, 126

Hwang, U., Hughes, J. P., Canizares, C. R., & Markert, T. H. 1993, ApJ, 414, 219

Itoh, H. 1979, PASJ, 31, 541

Kahn, S. M., Gorenstein, P., Harnden, F. R. & Seward, F. D. 1985, ApJ, 299, 821

Lampton, M., Margon, B., & Bowyer, S. 1976, ApJ, 208, 177

Landau, L. D., & Lifshitz, E. M. 1974, Fluid Mechanics, Pergamon Press.

Lotz, W., 1967, ApJS, 14, 207

Masai, K. 1984, Ap&SS, 98, 367

Masai, K. 1994, ApJ, 437, 770

McKee, C. F., & Cowie, L. L. 1975, ApJ, 195, 715

McKee, C. F., & Hollenbach, D. J. 1980, Ann. Rev. A&A, 18, 219

Mewe, R., & Gronenschild, E. H. B. M. 1981, A&AS, 45, 11

Myata, E., Tsunemi, H., Pisarski, R., & Kissel, S. E. 1994, PASJ, 46, L101

Murphy, D. C., & May, J. 1991, A&A, 247, 202

Press, W. H., Flannery, B. P., Teukolsky, S. A., Vetterling, W. T. 1986, Numerical Recipes, Cambridge University Press

Raymond, J. C. 1988, in Hot Thin Plasmas in Astrophysics, R. Pallavicini ed, Kluwer Academic Publisher, 3-20

Raymond, J. C. 1989, private communication

Raymond, J. C., & Smith, B. W. 1977, ApJS, 35, 419

Reale, F., Peres, G., & Serio, S. 1990, Nuovo Cimento B, 105, 1235

Sedov, L. 1959, Similarity and Dimensional Methods in Mechanics, New York, Academic Press

Shull, M. J., van Steenberg, M. 1982, ApJS, 48, 95

Summers, H. P. 1974. Culham Laboratory Internal Memo IM-367, Culham Laboratory, Ditton Park, Slough, England.

Taylor, G. I. 1950, Proc. R. Soc. London, A201, 159 and 175

Vancura, O., Raymond, J. C., Dwek, E., Blair, W. P., Long, K. S., & Foster, S. 1994, ApJ, 431, 188

Vedder, P. W., Canizares, C. R., Market, T. H., & Pradhan, A. K. 1986, ApJ, 307, 269

Weiler, K. W., & Panagia, N. 1980, A&A, 90, 269

Weiler, K. W., & Sramek, R. A. 1988, Ann. Rev. A&A , 26, 295

Woltjer, L. 1972, Ann. Rev. A&A, 10, 129

Yamauchi, S., Ueno, S., Koyama, K., Nomoto, S., Hayashida, K., Tsunemi, H., & Asaoka, I. 1993, PASJ, 45, 795

Yamauchi, S., Kawai, N., & Aoki, T. 1994, PASJ, 46, L109

Table 1: Number of counts in each spatial bin of the X-ray image

Annulus[a]	Angle[b]						
	a (15°)	b (20°)	c (25°)	d (30°)	e (35°)	f (40°)	g (45°)
1 (2.1-2.3)	128	7743	10195	7910	6594	1723	0
2 (2.3-2.5)	7244	17937	18409	15876	10865	6769	2183
3 (2.5-2.7)	16267	23813	18742	15233	11287	11529	9115
4 (2.7-2.9)	6454	13618	20583	22399	9457	8101	8954
5 (2.9-3.0)	3512	7429	16938	26930	9489	4045	4680
6 (3.0-3.2)	6063	8830	7182	6552	8960	5182	4675
7 (3.2-3.5)	1804	2294	2493	3280	5473	5701	3206

a - Distance in degrees from the Vela Pulsar.
b - Position angles measured in degrees where 0° is the North direction (top in Figure 2, Paper I).

Table 2: Statistical indetermination on best-fit parameter for the NEI model[a]

Map	Minimum Err.	Typical Err.	Maximum Err.
Temperature [keV]	0.03	0.05	0.1
Ionization time [log yr cm^{-3}]	0.5	0.7	1.3[b]

a - The errors indicated ($\pm\Delta$) have been computed at the 99% confidence level by a joint search on two interesting parameters. Minimum error refers to the bins with the highest count statistics ($\sim$ 25000 counts), typical errors refers to bins with $\sim$ 15000 counts, and maximum error to those with low count statistics ($\sim$ 5000 counts).
b - In some of the spatial bins, the ionization time is unconstrained at the chosen confidence level.

Table 3: Best-fit parameters and derived quantities for the "T3 bins"

Name	N_H (cm^{-2})[b]	T (keV)[a]	$\log\tau$ (yr cm^{-3})[a]	EM (cm^{-5})[b]	n (cm^{-3})[b]	p (dyn cm^{-2})[b]
c7	1.4×10^{20}	0.15-0.40	> 2.4	$10^{12.07}$	0.21	8.3×10^{11}
d6	0.6×10^{20}	0.15-0.35	> 2.5	$10^{11.69}$	0.14	7.8×10^{11}
e7	1.2×10^{20}	0.10-0.30	0.0-1.0 & > 2.5	$10^{11.80}$	0.13	5.3×10^{11}

a - range estimated by means of 99% level confidence contours in the $T - \tau$ plane (two interesting parameters).
b - best-fit values.

Figure Captions

Fig. 1: X-ray emissivity versus ionization time at various temperatures in the 0.1-2.0 keV band computed with our STNEI model, both unfolded (*left*) and folded with the PSPC instrumental response (*right*). The folded curves have been computed by generating the PSPC spectra for each model grid point and summing on SASS channels 3-30. Each curve is labelled with the corresponding temperature in keV.

Fig. 2: From left to right: *(a)* Grey scale Map of the observed counts in the 0.1-2.0 keV band. The data have been sampled on a spatial grid reflecting the circular symmetry of the Vela SNR emission as a whole, and yielding few thousand counts per bin for an optimal parameter restoration with the STNEI model. *(b)* χ^2 map. The grey scale top is at $\chi^2 = 36$ which is the threshold at the 95% confidence level. Spatial bins with $\chi^2 > 36$ are not displayed.

Fig. 3: Top: *(a):* PSPC spectrum at position *e6* with the correspondent best-fit STNEI spectrum, parameters, and residuals. We also report the confidence contours (68, 90 and 99% level) in the $T - \log \tau$ plane. The unfolded best-fit spectrum is shown on the right. Bottom: *(b):* Same as above but for bin *c7*.

Fig. 4: PSPC spectrum at position *d3* as an example of spectrum not fitted by our model.

Fig. 5: From top left to bottom right: *(a)* Temperature map. *(b)* Ionization time map. Units and ranges are also indicated for each map.

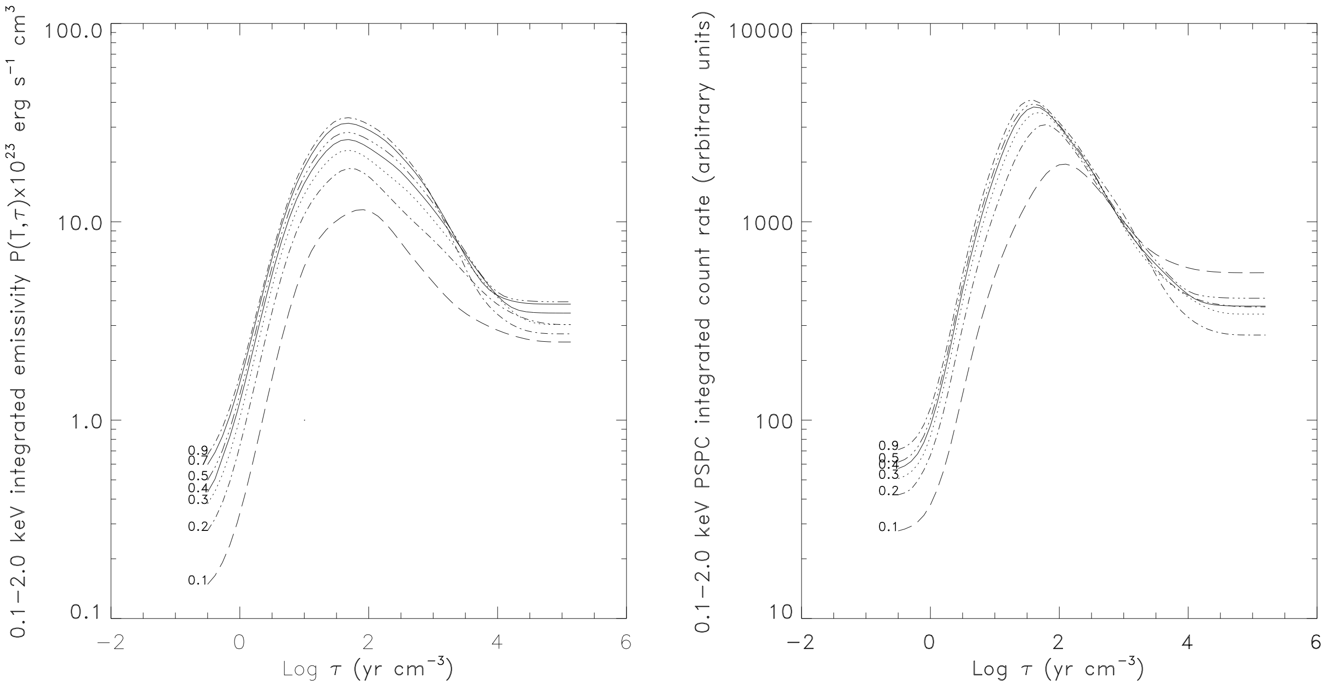
0.1−2.0 keV integrated emissivity P(T,τ)x10^23 erg s^-1 cm^3
100.0
10.0
1.0
0.1
−2
0
2
4
6
Log τ (yr cm^-3)
0.9
0.7
0.5
0.4
0.3
0.2
0.1
0.1−2.0 keV PSPC integrated count rate (arbitrary units)
10000
1000
100
10
−2
0
2
4
6
Log τ (yr cm^-3)
0.9
0.5
0.4
0.3
0.2
0.1

Figure 1:

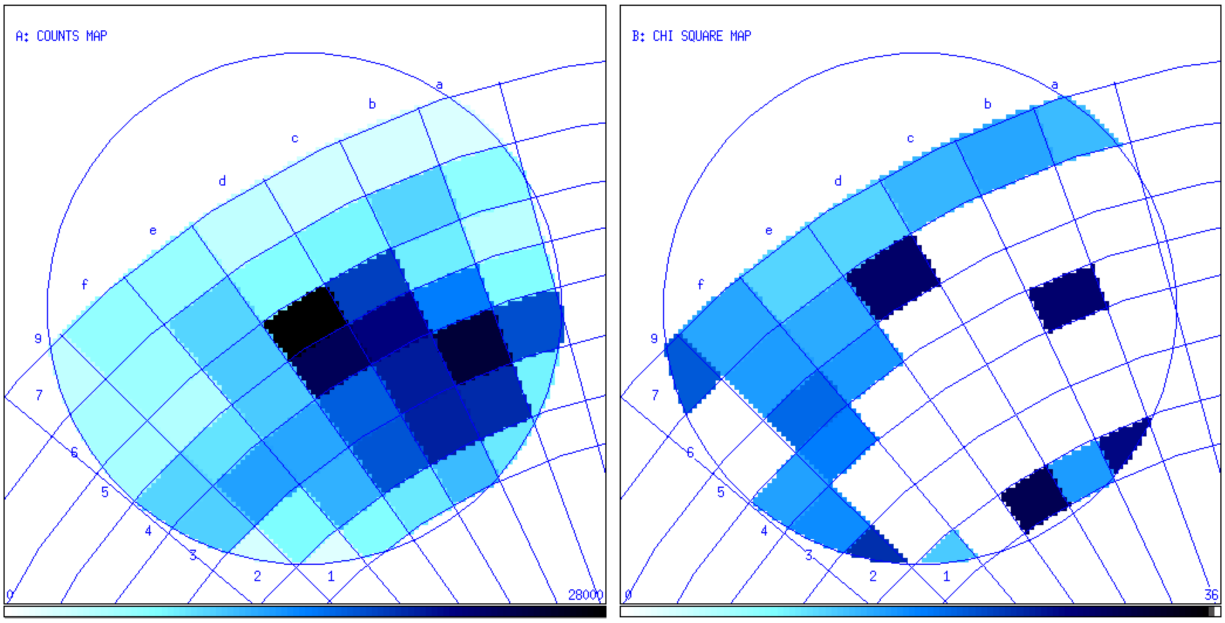

Figure 2:

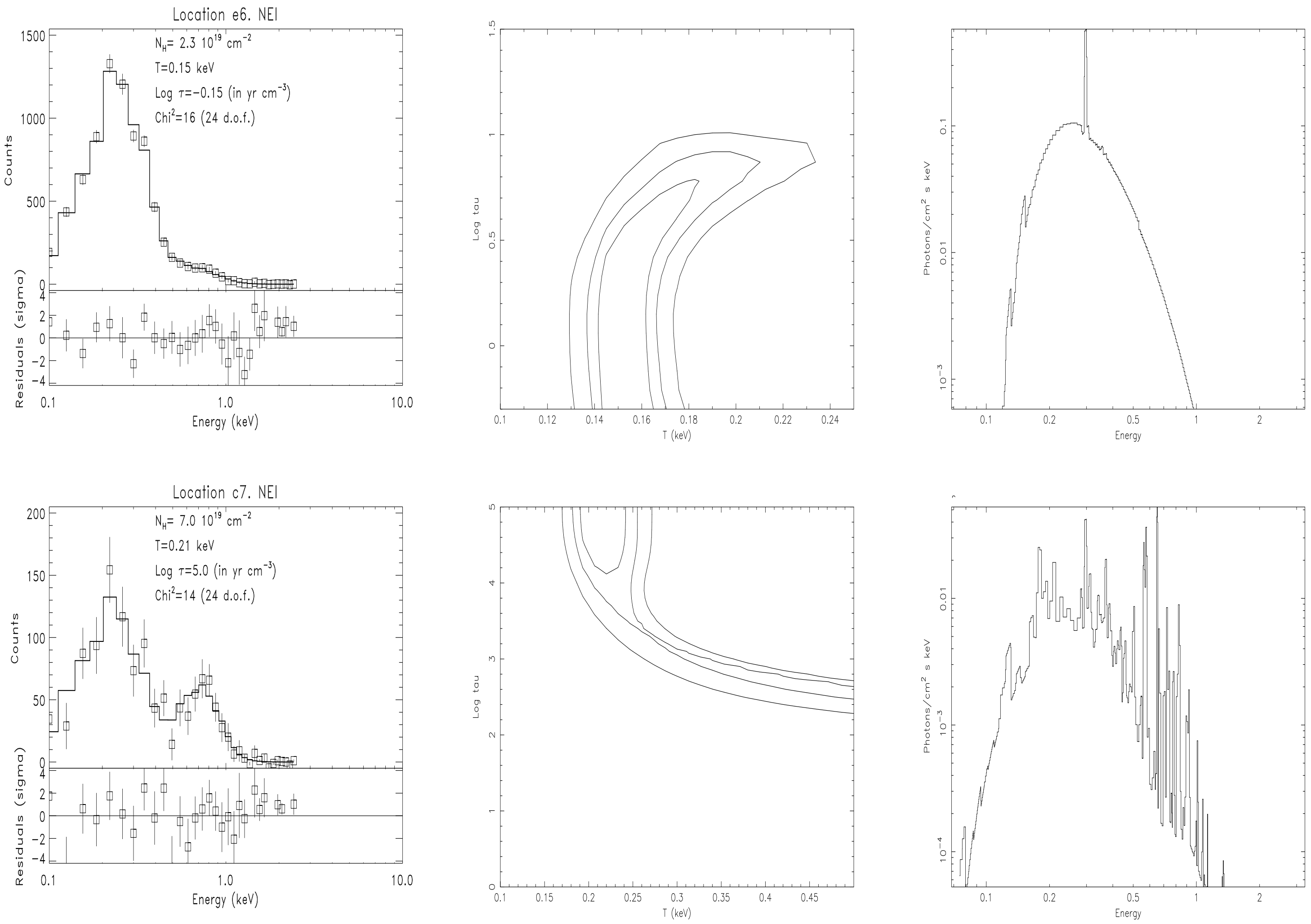
Location e6. NEI
N_H= 2.3 10^{19} cm^{-2}
T=0.15 keV
Log τ=-0.15 (in yr cm^{-3})
Chi^2=16 (24 d.o.f.)
Counts
Residuals (sigma)
Energy (keV)
Log tau
T (keV)
Photons/cm^2 s keV
Energy
Location c7. NEI
N_H= 7.0 10^{19} cm^{-2}
T=0.21 keV
Log τ=5.0 (in yr cm^{-3})
Chi^2=14 (24 d.o.f.)
Counts
Residuals (sigma)
Energy (keV)
Log tau
T (keV)
Photons/cm^2 s keV
Energy

Figure 3:

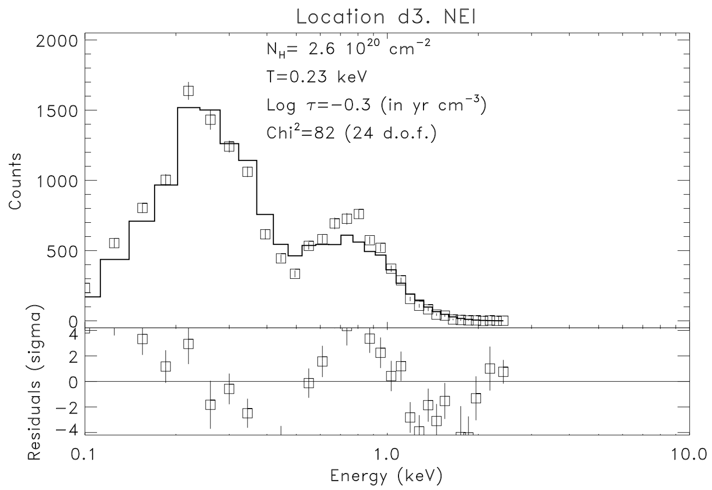

Location d3. NEI
N_H= 2.6 10^20 cm^-2
T=0.23 keV
Log τ=−0.3 (in yr cm^-3)
Chi^2=82 (24 d.o.f.)
Counts
Residuals (sigma)
Energy (keV)

Figure 4:

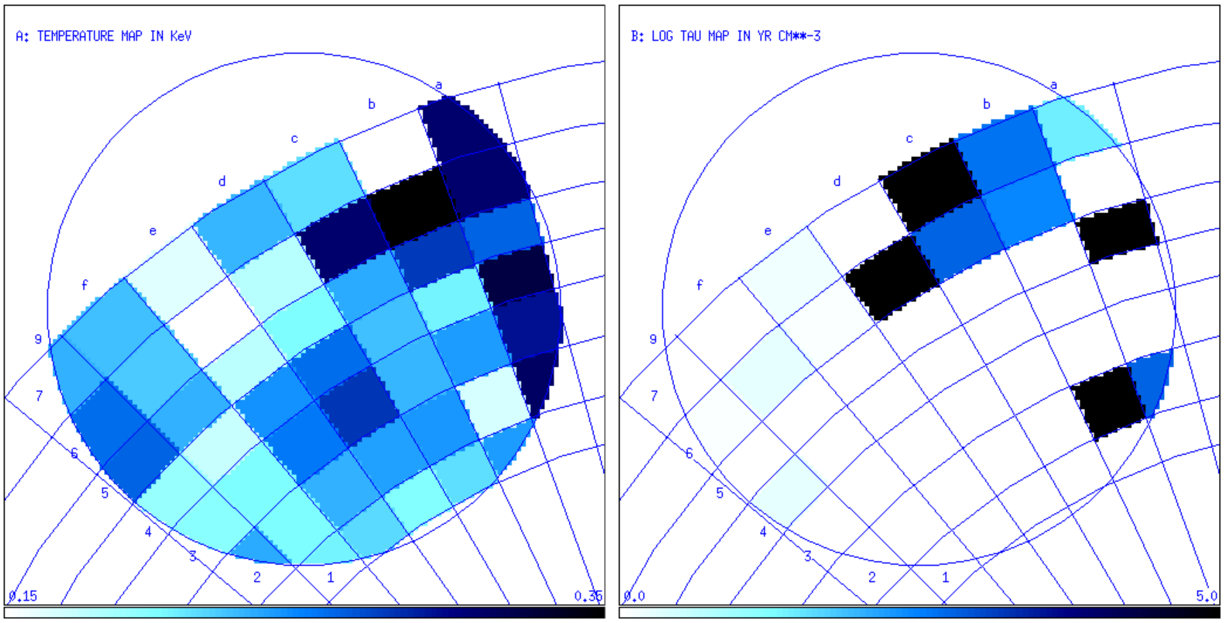
A: TEMPERATURE MAP IN KeV
a
b
c
d
e
f
9
7
6
5
4
3
2
1
0.15
0.35
B: LOG TAU MAP IN YR CM**-3
a
b
c
d
e
f
9
7
6
5
4
3
2
1
0.0
5.0

Figure 5: